Noninvasive Optical Measures of CBV, StO_2, CBF Index, and $rCMRO_2$ in Human Premature Neonates' Brains in the First Six Weeks of Life

Nadège Roche-Labarbe,[1]* Stefan A. Carp,[1] Andrea Surova,[1] Megha Patel,[1] David A. Boas,[1] P. Ellen Grant,[2] and Maria Angela Franceschini[1]

[1]*Martinos Center for Biomedical Imaging, Massachusetts General Hospital/Harvard Medical School, Charlestown, Massachusetts*
[2]*Department of Radiology, Massachusetts General Hospital, Boston, Massachusetts*

Abstract: With the causes of perinatal brain injuries still unclear and the probable role of hemodynamic instability in their etiology, bedside monitoring of neonatal cerebral hemodynamics with standard values as a function of age are needed. In this study, we combined quantitative frequency domain near infrared spectroscopy (FD-NIRS) measures of cerebral tissue oxygenation (StO_2) and cerebral blood volume (CBV) with diffusion correlation spectroscopy (DCS) measures of a cerebral blood flow index (CBF_{ix}) to test the validity of the CBV-CBF relationship in premature neonates and to estimate cerebral metabolic rate of oxygen ($rCMRO_2$) with or without the CBF_{ix} measurement. We measured 11 premature neonates (28–34 weeks gestational age) without known neurological issues, once a week from one to six weeks of age. In nine patients, cerebral blood velocities from the middle cerebral artery were collected by transcranial Doppler (TCD) and compared with DCS values. Results show a steady decrease in StO_2 during the first six weeks of life while CBV remains stable, and a steady increase in CBF_{ix}. $rCMRO_2$ estimated from FD-NIRS remains constant but shows wide interindividual variability. $rCMRO_2$ calculated from FD-NIRS and DCS combined increased by 40% during the first six weeks of life with reduced interindividual variability. TCD and DCS values are positively correlated. In conclusion, FD-NIRS combined with DCS offers a safe and quantitative bedside method to assess CBV, StO_2, CBF, and $rCMRO_2$ in the premature brain, facilitating individual follow-up and comparison among patients. A stable CBV-CBF relationship may not be valid for premature neonates. *Hum Brain Mapp 31:341–352, 2010.* © 2009 Wiley-Liss, Inc.

Key words: premature neonates; brain hemodynamics; near-infrared spectroscopy; diffuse correlation spectroscopy; cerebral blood flow; cerebral oxygen consumption; brain development

INTRODUCTION

Because of the expansion of neonatal intensive care and assisted reproductive technology, a significant and increasing number of neonates are born prematurely [Martin et al., 2009]. These patients are at special risk for cerebral injuries such as hypoxia-ischemia, stroke, and periventricular leukomalacia, any of which can be associated with long-term epilepsy or neurological deficits [Kiechl-Kohlendorfer et al., 2009]. With the cause of these disorders still unclear and the probable role of hemodynamic instability in their etiology, it is essential to develop bedside methods to monitor cerebral hemodynamic variables. Although the

Additional Supporting Information may be found in the online version of this article.

Contract grant sponsor: NIH; Contract grant number: R01 HD42908.

*Correspondence to: Nadège Roche-Labarbe, Martinos Center for Biomedical Imaging, Massachusetts General Hospital, Bdg 149, 13th St, Charlestown MA 02129. E-mail: nadege@nmr.mgh.harvard.edu

Received for publication 6 May 2009; Revised 26 June 2009; Accepted 29 June 2009

DOI: 10.1002/hbm.20868

Published online 31 July 2009 in Wiley InterScience (www.interscience.wiley.com).

emphasis has been on supportive care [Perlman, 2006], there is an increasing effort to organize clinical trials and test new agents [Marret et al., 2008]. However, there are very few tools available for routine bedside assessment of neonatal brain health, and they do not assess local cerebral hemodynamics. While amplitude-integrated electroencephalography (aEEG), head ultrasound (US), and transcranial Doppler (TCD) remain the most common bedside methods, the value of aEEG is still unclear [Shellhaas et al., 2007], US is notoriously insensitive to brain injury [Blankenberg et al., 2000], and TCD estimates blood flow only in the main arteries.

Our current understanding of metabolic and vascular regional brain development in infants is derived from positron emission tomography (PET), single photon emission computed tomography (SPECT), and functional magnetic resonance imaging (fMRI) studies. Using ^{18}F-FDG PET, a correlation has been established between glucose utilization and behavioral and neurophysiological maturation [Chugani and Phelps, 1986]. In neonates, glucose uptake is highest in the sensorimotor cortex, with generally low functional activity over most of the other regions. During the second and third months of life, glucose uptake begins to increase in the parietal, temporal and primary visual cortices, coinciding with improvements in motor and visual skills [Amiel-Tison and Grenier, 1986; Bayley, 1993] as well as with changes in the EEG response to stimuli [Kellaway, 2003]. Other investigators have observed similar developmental changes in cerebral blood flow (CBF) using $H_2{}^{15}O$ PET [Altman et al., 1988] and ^{123}I-IMP SPECT [Tokumaru et al., 1999]. Regional myelination changes also correlate with glucose uptake and increases in CBF [Peterson et al., 2003], suggesting either higher energy demand during myelination or, more likely, increased cerebral activity in myelinating regions. However, these techniques are rarely performed because they cannot be used at the bedside, and PET and SPECT present a risk of radiation exposure.

There have been a few previous reports of cerebral metabolic rate of oxygen ($CMRO_2$) in neonates; $CMRO_2$ was reported higher in term neonates compared to premature neonates [Altman et al., 1988; Elwell et al., 2005; Skov et al., 1993; Yoxall and Weindling, 1998]. However, these studies had small samples of subjects with injuries such as hyaline membrane disease or intraventricular hemorrhage in the premature population and suspicion of hypoxic ischemic injury in the term infants.

To better understand normal hemodynamic development and to promptly identify pathological development, a safe portable technique for quantitative, reliable monitoring of local cerebral blood volume (CBV), cerebral blood flow, oxygen saturation (StO_2), and $CMRO_2$ is needed.

Near infrared spectroscopy (NIRS) provides bedside monitoring of CBV and StO_2. It is portable, noninvasive and safe because it uses nonionizing radiation and emits less energy than a head ultrasound [Bozkurt and Onaral, 2004; Ito et al., 2000]. For this reason, NIRS is particularly adapted for use in neonates and infants, and was first applied to the study of the neonatal brain in the mid-1980s [Benaron et al., 1992; Brazy et al., 1985; Wyatt et al., 1986]. Continuous wave near infrared spectroscopy (CW-NIRS) has now become a widespread noninvasive measure of oxy- and deoxy-hemoglobin concentrations (HbO and HbR) [Carlsson et al., 2008; Watanabe et al., 2008; Zaramella et al., 2007]. However, it does not allow absolute measurements.

There have been attempts to optically measure regional CBF in neonates using NIRS, but either oxy-hemoglobin was used as a tracer [Edwards et al., 1988; Elwell et al., 2005; Meek et al., 1998; Noone et al., 2003], a method applicable only on ventilated infants, or indocyanine green was used as a tracer [Patel et al., 1998], with the injection of the dye not performed in healthy infants for ethical reasons.

The absence of absolute hemoglobin concentration and oxygenation measurements and of reliable CBF assessment has been a major obstacle to the successful clinical application of NIRS. The lack of quantification prevents estimation of standard values and efficient comparison of at-risk neonates with normal neonates [Nicklin et al., 2003].

Advances have been made to address the issue of absolute measurements by using time-domain and frequency-domain spectroscopy (TD-NIRS and FD-NIRS, respectively), both of which allow absolute quantification of StO_2 and CBV [Fantini et al., 1995; Hamaoka et al., 2000]. Although TD-NIRS has had limited clinical use so far because of instrument complexity [Benaron et al., 1994; Hebden et al., 2002], the development of FD-NIRS systems has increased quantitative accuracy while maintaining simplicity [Ijichi et al., 2005; Zhao et al., 2005]. Recently, FD-NIRS has been used successfully to measure the evolution of CBV, StO_2, and $CMRO_2$ over the first year of normal brain development [Franceschini et al., 2007].

Regarding CBF, a recently developed method of diffuse correlation spectroscopy (DCS) provides a measure of tissue perfusion based on the movement of scatterers (i.e., blood cells) inside the tissue [Boas and Yodh, 1997; Cheung et al., 2001]. It has proven a valid assessment of CBF changes in the brain [Durduran et al., 2004b; Li et al., 2005].

In this study our aims were to (1) establish standard baseline values of CBV and StO_2 and their evolution during the first six weeks of life in premature neonates with neither brain injury nor severe cardiovascular issues, (2) evaluate the relevance of DCS for baseline CBF assessment in neonates, and (3) determine whether $CMRO_2$ changes could be better assessed with combined FD-NIRS and DCS rather than a hypothetical CBV-CBF relationship [Grubb et al., 1974].

MATERIALS AND METHODS

Subjects

We recruited from the NICU or the Well Baby Nursery at the Massachusetts General Hospital (MGH) 11 premature

TABLE I. Subjects information

ID	Birth weight (g)	GA (weeks)	Sex
1	1,970	33 0/7	M
2	1,900	33 0/7	F
3	1,780	33 0/7	M
4	1,330	27 6/7	M
5	1,220	27 6/7	M
6	1,355	30 6/7	M
7	1,230	30 6/7	F
8	2,070	33 4/7	F
9	1,030	28 2/7	M
10	1,120	28 1/7	F
11	1,490	29 5/7	F
Extra patients for DCS-TCD comparison			
12	1,090	28 4/7	F
13	1,310	32 5/7	M
14	820	25 5/7	M

neonates, 28 to 34.5 weeks gestational age (wGA), with no clinical suspicion of brain injury (Table I). All of them had APGAR scores between 7 and 9 after 5 min. For this initial study, some subjects requiring respiratory support but with normal arterial saturation were included (see Supporting Information table online for detailed clinical information). We measured each baby once a week from one to six weeks of age (ages in days were rounded off to the nearest week). Our Institutional Review Board approved the study and parents signed an informed consent.

Techniques

For frequency-domain near infrared spectroscopy, we used a customized commercial frequency-domain oximeter from ISS Inc., Champaign, IL, USA. It has 16 laser sources, emitting at eight wavelengths with two redundant pairs (659, 2 × 685, 755, 778, 798, and 2 × 825 nm) and two PMT detectors (http://www.iss.com/products/oxiplex/). The sources were modulated at 110 MHz; the detectors at 110 MHz plus 5 kHz to achieve heterodyne detection. The lasers were rapidly multiplexed in sequence, so only one source was on at any given time (for 10 ms), allowing separation by software on the detector side.

For diffuse correlation spectroscopy, we used a custom-built instrument similar to the system developed by Drs. Arjun Yodh and Turgut Durduran at the University of Pennsylvania [Cheung et al., 2001; Durduran et al., 2004b; Li et al., 2005]. It consists of one long coherence length laser source at 785 nm (CrystaLaser, Reno, NV, USA) and four photon-counting avalanche photodiodes (APD) as detectors (Perkin-Elmer, Quebec, Canada). The individual counting signals were converted to temporal intensity auto-correlation functions by an eight-channel correlator (http://www.correlator.com/).

Both instruments were compact enough to be moved on a small cart to the infant's bedside in the hospital. They were controlled by the same laptop and operated in sequence.

Two groups of eight NIRS lasers (~ 1 mW power each) were combined into two source fiber bundle, and each detector coupled to a fiber bundle. The NIRS fiber bundles (each 2.5 mm diameter) were arranged in a row in a black rubber probe ($5 \times 2 \times 0.5$ cm^3) with source-detector distances of 1, 1.5, 2, and 2.5 cm (Fig. 1C). Multiple distances are necessary to quantify absorption and scattering coefficients with this system [Fantini et al., 1995]. Because we separately measured absorption and scattering there was no need to assume a path length factor at each wavelength as is done with CW systems. The source-detector separations we chose (from 1 to 2.5 cm) are adequate for a depth penetration of about 1 cm, which includes the cerebral cortex in neonates [Fabbri et al., 2004; Franceschini et al., 1998].

The DCS laser (50 mW power) was coupled to a multimode optical fiber (62.5 μm diameter) and diffused at the fiber tip to a 3-mm spot; the DCS detectors were coupled to 5.6 μm diameter optical fibers which achieved single mode operation at 785 nm. The fibers were arranged in a second row parallel to the NIRS bundles, with the same source-detector separations (Fig. 1C). For this paper, only the 1.5 cm pair was used in the results, because it was the largest distance that provided a good signal-to-noise ratio in all babies.

Acquisition Protocol

FD-NIRS and DCS were performed in turn at bedside (Fig. 1A). For both, measurements were obtained from up to seven areas of the head (Fp1, FpZ, Fp2, T3, T4, CP3, and CP4, according to the 10–20 system, Fig. 1B). The optical probe was held in each location for 8 s of data acquisition. Measurements with each instrument were repeated up to

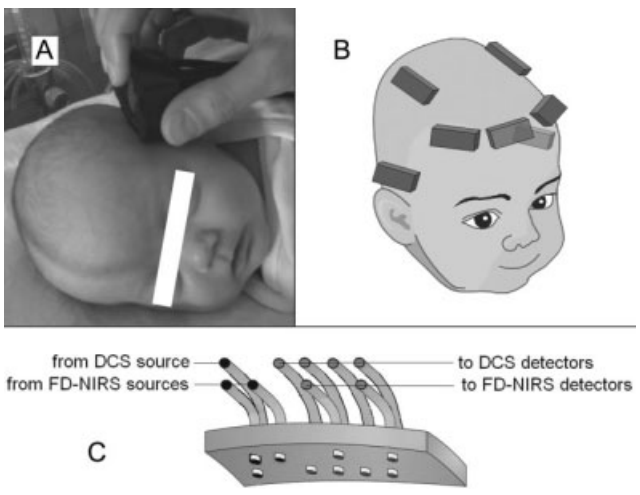

Figure 1.
A: Picture of a subject during a measurement. **B:** Locations of recording on the subject's head. **C:** Schema of the probe.

three times in each location, with the probe repositioned in order to make up for local inhomogeneities such as hair and superficial large vessels and thus ensure that the measurement was representative of the underlying brain region. The total number of positions and repetitions depended on the cooperation of the subject and the presence of other medical devices on the head. Total examination time was ~45 min. Hemoglobin counts were taken from clinical reports and SaO_2 was obtained from monitoring devices.

DCS-TCD Comparison

To validate DCS measurements, we collected TCD measurements of cerebral blood velocities (PS, peak systolic; ED, end diastolic) for the middle cerebral artery, which were acquired for clinical reasons in nine patients within a day of our DCS measurement. We then compared them with DCS values. Among these patients, six were participants in the main study (patients 4, 5, 6, 7, 10, and 11); each provided several DCS-TCD time points. The remaining three patients had only one DCS measurement, and for that reason were not part of the longitudinal optical study. These three infants were also stable premature neonates without brain injury (see Table I); each provided one DCS-TCD time point.

NIRS Data Processing

We used the amplitude and phase data collected at each wavelength to determine average absorption and scattering coefficients using the multi-distance frequency-domain method [Fantini et al., 1995].

To analyze the FD-NIRS data in a standardized fashion we developed an automated data analysis routine, which includes data quality assessment and data rejection based on previously established statistical criteria. In particular we used the following procedure:

For each wavelength we discarded all data points with $R^2 < 0.97$ for the fit of the raw optical data (amplitude and phase) to the light transportation model; if more than 80% of data points were discarded, all data for that wavelength were discarded; if more than two wavelengths had to be discarded, one source-detector distance was discarded and the data point and wavelength selection steps were repeated; if more than one distance had to be discarded, the whole measurement was discarded. In addition, the whole measurement was discarded if $P > 0.02$ for the fit of the absorption coefficients with the hemoglobin spectra or for a linear fit of the reduced scattering coefficient versus wavelength. Using these objective rejection criteria, we were able to discard data affected by hair, bad coupling to the head, bending of the probe, and motion artifacts, and thus retain only the highest quality data for further analysis.

We derived HbO and HbR by fitting the absorption coefficient at our wavelengths with the hemoglobin spectra using the extinction coefficients reported in the literature [Wray et al., 1988] and a 75% concentration of water [Wolthuis et al., 2001], and from them calculated total hemoglobin concentration HbT (μMol) and StO_2:

$$\mathrm{HbT} = \mathrm{HbO} + \mathrm{HbR} \tag{1}$$

$$\mathrm{StO_2} = \mathrm{HbO}/\mathrm{HbT} \tag{2}$$

CBV was calculated using the following equation [Takahashi et al., 1999]:

$$\mathrm{CBV} = \frac{(\mathrm{HbT} \times \mathrm{MW_{Hb}})}{\mathrm{HGB} \times \mathrm{D_{bt}}} \tag{3}$$

where CBV is in ml/100 g, HbT is in μMol, MW_{Hb} (64,500 g/Mol) is the molecular weight of hemoglobin, D_{bt} (1.05 g/ml) is the brain tissue density [Kretschmann et al., 1986] and HGB (g/dl) is hemoglobin concentration in the blood. For 20% of measurements HGB was not available in clinical charts, in which case standard normal values for HGB for age were used [de Alarcón and Werner, 2005; Wolff and Goodfellow, 1955]. Uncertainties in the above physiologic parameters have previously been reported [Franceschini et al., 2007].

To estimate relative $CMRO_2$ ($rCMRO_2$) from FD-NIRS only, we used the relation

$$\mathrm{CMRO_2}\,\frac{\mathrm{HGB} \cdot \mathrm{CBF} \cdot (\mathrm{SaO_2} - \mathrm{SvO_2})}{\mathrm{MW_{hb}}} \tag{4}$$

where SaO_2 is the arterial and SvO_2 the venous hemoglobin oxygenation.

We worked from the assumption that:

$StO_2 = aSaO_2 + bSvO_2$, with $a + b = 1$ [Watzman et al., 2000] and a and b are constants.

Next we assumed a constant power law relation between changes in CBF and CBV

$$\frac{\mathrm{CBF}}{\mathrm{CBF_o}} = \left(\frac{\mathrm{CBV}}{\mathrm{CBVCBV_o}}\right)^{\beta} \tag{5}$$

with β 2.6 [Brown et al., 2003; Grubb et al., 1974] and the subscript "$_o$" indicating the reference values.

Finally, we obtained

$$\mathrm{rCMRO_2} = \frac{\mathrm{CMRO_2}}{\mathrm{CMRO_{2o}}} = \frac{\mathrm{HGB}}{\mathrm{HGB_o}} \cdot \left(\frac{\mathrm{CBV}}{\mathrm{CBV_o}}\right)^{\beta} \cdot \left(\frac{\mathrm{SaO_2} - \mathrm{StO_2}}{\mathrm{SaO_{2o}} - \mathrm{StO_{2o}}}\right) \tag{6}$$

$rCMRO_2$ was calculated as the ratio between the subject's values and the average of all subjects' first week values.

Because the reference values are the average of all subjects' first week values, and not the subject's own first week value, the initial average of all subjects is not exactly one.

In each infant for each measurement session, multiple measurements in the same location were averaged together, and for this article results were averaged over all positions. We verified that results are reliable when only one location is considered by comparing results using only frontal or only parietal measurements, which did not produce significant differences.

DCS Data Processing

Diffuse correlation spectroscopy offers a measure of tissue perfusion that depends on both the movement of scatterers inside the tissue and the tissue optical properties [Boas and Yodh, 1997; Cheung et al., 2001]. To maximize accuracy we calculated the actual optical absorption and scattering coefficients at 785 nm by interpolating from the FD-NIRS measurements.

DCS data comprise a set of intensity auto-correlation curves (over a delay time range of 200 ns ~1s in our case) acquired sequentially, about once per second. The diffusion correlation equation offers the theoretical framework for analyzing our data. As detailed in [Boas et al., 1995; Boas and Yodh, 1997] and further validated in [Cheung et al., 2001; Culver et al., 2003; Durduran et al., 2004a; Durduran et al., 2005] the normalized intensity temporal auto-correlation function, $g_2(\tau)$, is given by:

$$g_2(r_s, r_d, \tau) = \left(1 + \exp\left(-(3\mu_s'\mu_a + (P_{RBC}\mu_s')^2 k_0^2 \langle \Delta r^2(\tau)\rangle)^{1/2} |r_s - r_d|\right)\right) \quad (7)$$

where the source is at position r_s, the detector is at position r_d, the correlation time is τ, the reduced scattering coefficient is μ_s', the absorption coefficient is μ_a, the wave number for the laser light is k_o, $\langle \Delta r^2(\tau)\rangle$ is the mean square displacement of the moving scattering particles (i.e., the red blood cells) where $\langle \ldots \rangle$ indicates an ensemble average, and P_{RBC} is the probability of scattering from a moving red blood cell instead of the static tissue matrix. The most common model for the mean square displacement of the moving particles is Brownian motion:

$$\langle \Delta r^2(\tau)\rangle = 6 D_B \tau \quad (8)$$

where D_B is the Brownian diffusion coefficient. Since P_{RBC} is generally unknown, the two parameters are usually grouped together ($D_B P_{RBC}$) to form a blood flow index hereafter referred to as CBF_{ix}, which has been shown to follow tissue perfusion quite accurately [Yu et al., 2005].

To obtain the blood flow index, we fit Eq. (7) to the measured temporal auto-correlation functions, and, as we did in analyzing the FD-NIRS data, we reject measurements that do not met the objective criteria described below in order to maintain good data quality.

First, we discarded correlation curves for which the tail (large τ) of the fitting curve differed from 1 by more than 0.02, the cumulative variation among the 3 first points of the curve was more than 0.1, or the average value of the 3 first points of the curve was more than 1.6 (all indicative of high measurement noise, as a $g_2(\tau)$ curve obtained using randomly polarized light reaches a maximum of 1.5 at $\tau = 0$ and decays to 1 for large τ values [Kirkpatrick et al., 2008]). If more than 50% of curves were discarded, the whole set was discarded. Finally, we used only sets for which the fit values from the kept curves had a coefficient of variation (COV, standard deviation/mean ratio) <15%.

Although measurements of relative changes in blood flow index have previously been reported, for example during functional measurements [Durduran et al., 2004b] or cancer therapy monitoring [Zhou et al., 2007], the present work is one of the first attempts to use DCS to obtain absolute blood flow index measurements. As described by Yu et al. [2005] the DCS blood flow index is proportional to tissue perfusion. To compare measurements taken at different locations, times, and subjects, we made the assumption that the proportionality factor is constant within location, ages, and subjects.

We assessed the reproducibility of the DCS measurements by calculating the COV for a set of 10 measurements on a 1% intralipid liquid phantom using the probe described above. COV was 12%. We then ran the same calculation for each set of three measurements in each location for every subject included in this study. This intralocation COV was 13 ± 2%. We believe the slightly larger COV in vivo is because of the fact that we do not reposition the probe exactly in the same location, but rather in a slightly different area, to obtain an average value at that head location. Inhomogeneities in the underlying vasculature may be responsible for the higher COV of CBF_{ix} in vivo. For comparison, the error we obtain with FD-NIRS is 11 ± 1% for HbT and 4 ± 1% for StO_2. These errors are significantly smaller than the changes of StO_2, CBF_{ix}, and $rCMRO_2$ with age (see Results).

As for NIRS, in each infant for each measurement session DCS measurements in the same location were averaged together, and for this article results were averaged over all positions.

To estimate relative $CMRO_2$ ($rCMRO_2$) from combined DCS and FD-NIRS measures, without assuming a CBV-CBF relationship [Eq. (5)], we used the relation:

$$rCMRO_2 = \frac{CMRO_2}{CMRO_{2o}} = \frac{HGB}{HGB_o} \cdot \left(\frac{CBFix}{CBFix_o}\right)^{\beta} \cdot \left(\frac{SaO_2 - StO_2}{SaO_{2o} - StO_{2o}}\right) \quad (9)$$

We used Matlab® (http://www.mathworks.com/products/matlab/) for all data processing, Excel® (http://office.microsoft.com/en-us/excel/) for plotting and

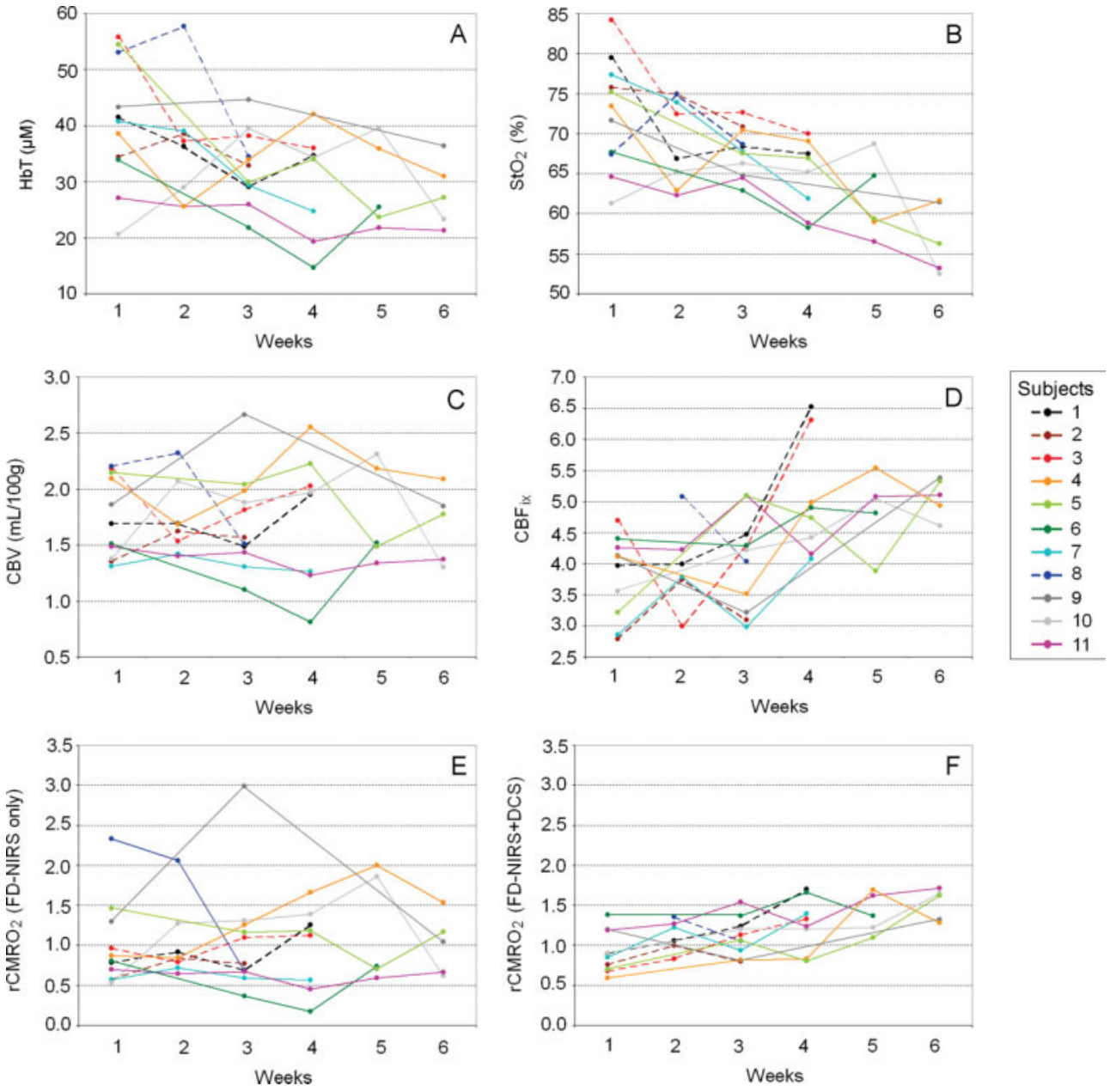

Figure 2.
Individual traces as a function of age. **A:** HbT. **B:** StO_2. **C:** CBV. **D:** CBF_{ix}. **E:** $rCMRO_2$ estimated from FD-NIRS only. **F:** $rCMRO_2$ calculated by combining FD-NIRS and DCS. Dotted lines are subjects born after 32 wGA, solid lines for subjects born before 32 wGA.

Statistica® (http://www.statsoft.com/) for regressions and statistics.

RESULTS

In Figure 2 we plot individual traces of HbT, CBV, StO_2, CBF_{ix}, $rCMRO_2$ estimated from FD-NIRS only, and $rCMRO_2$ calculated by combining FD-NIRS and DCS as a function of age. We plot averages ±95% confidence intervals of these variables as a function of age in Figure 3. Because we had 11 subjects, the confidence intervals were calculated using Student's t table for small samples. For each average variable, we calculated and plotted the linear regression, with R^2 and P-value.

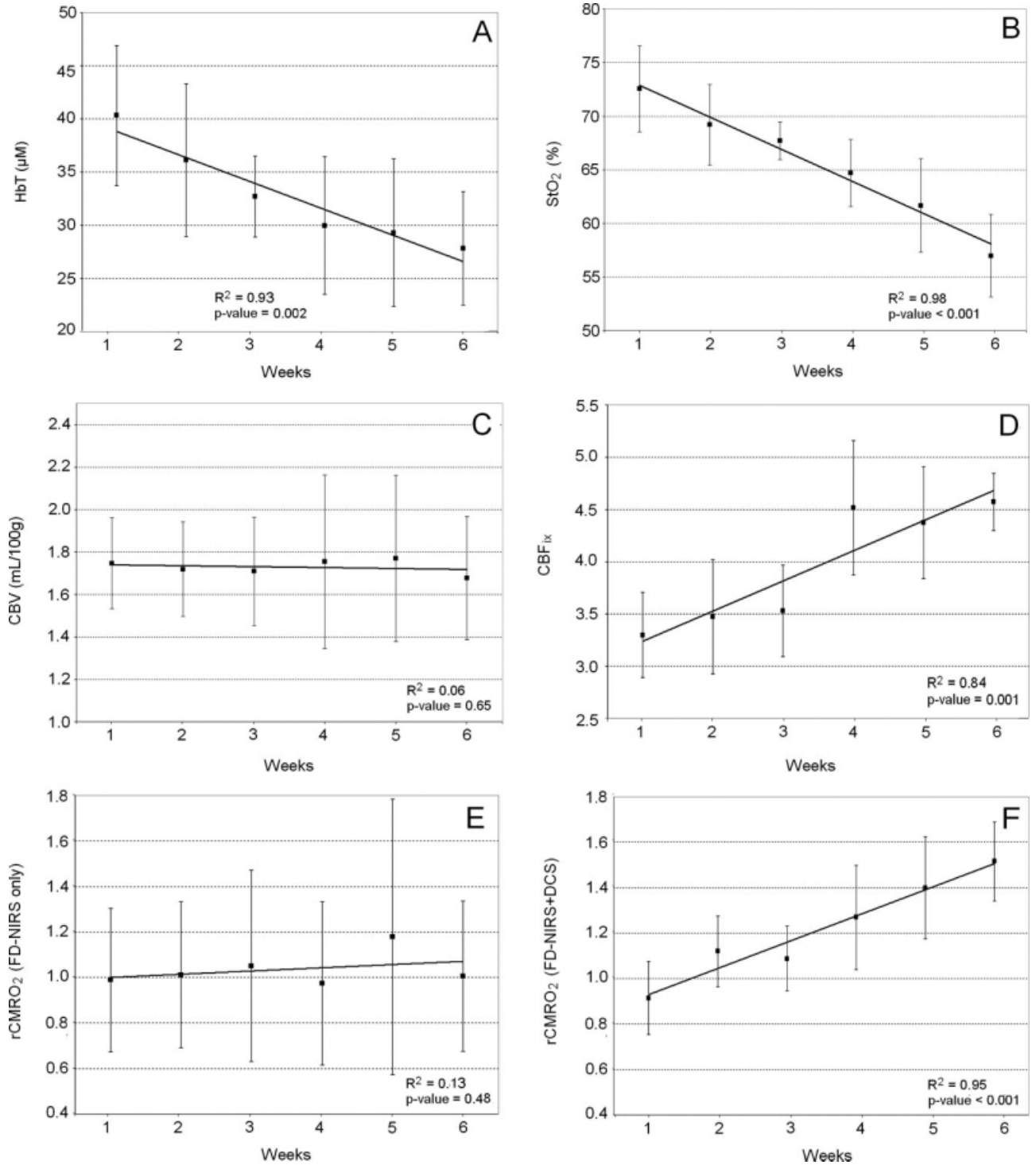

Figure 3.

Averages ±95% confidence intervals as a function of age. **A:** HbT. **B:** StO_2. **C:** CBV. **D:** CBF_{ix}. **E:** $rCMRO_2$ estimated from FD-NIRS only. **F:** $rCMRO_2$ calculated by combining FD-NIRS and DCS. Bold lines are linear regressions; R^2 and *P*-value of the regressions are in the bottom right corner of each graph.

Individual traces of HbT show a decrease during the first six weeks of life (Fig. 2A). The average HbT significantly decreases from 40 ± 7 to 28 ± 5 μM during this period (31% decrease, $R^2 = 0.93$, P-value = 0.002) (Fig. 3A).

Individual traces of StO_2 show a consistent decrease during the first six weeks of life (Fig. 2B). The average StO_2 significantly decreases from 73 ± 4% to 57 ± 4% during this period (21% decrease, $R^2 = 0.98$, P-value <0.001) (Fig. 3B).

In the contrary, individual traces of CBV do not show a consistent pattern of evolution across subjects during the first six weeks of life (Fig. 2C). The average CBV stays constant around 1.7 ± 0.3 ml/100 g during this period ($R^2 = 0.06$, P-value = 0.65) (Fig. 3C). This is consistent with previously reported values [Leung et al., 2004].

Individual traces of CBF_{ix} calculated from DCS show a consistent increase during the first six weeks of life (Fig. 2D). The average CBF_{ix} significantly increases from 3.3 ± 0.4 to 4.6 ± 0.3 during this period (28% increase, $R^2 = 0.84$, P-value = 0.001) (Fig. 3D).

Individual $rCMRO_2$ traces estimated from FD-NIRS alone do not show a consistent pattern of evolution across subjects during the first six weeks of life (Fig. 2E). On an average, $rCMRO_2$ estimated from FD-NIRS alone remains constant during this period 1.0 ± 0.4 ($R^2 = 0.13$, P-value = 0.48) and shows a large variation among subjects (average standard deviation = 0.52) (Fig. 3E).

Individual $rCMRO_2$ traces calculated by combining FD-NIRS and DCS show instead a strong increase with age during the first six weeks of life (Fig. 2F). On average, $rCMRO_2$ calculated by combining FD-NIRS and DCS increases from 0.9 ± 0.3 to 1.5 ± 0.2 (40% increase, $R^2 = 0.95$, P-value <0.001), and there is a much smaller variation between subjects than when using FD-NIRS alone (average standard deviation = 0.24) (Fig. 3F).

HbT and StO_2 seemed higher in neonates born after 32 wGA compared with neonates born before 31 wGA, for the first four weeks of life (data were missing for weeks 5 and 6 in the first group) (Fig. 2A,B). However, our small samples did not allow for statistics on this effect.

To validate the DCS measures of CBF, we plotted the average of PS and ED values from the TCD versus CBF_{ix} from the DCS in Figure 4. We also calculated and plotted the linear regression, with R^2 and P-value. This shows that DCS measurements are positively correlated ($R^2 = 0.28$, P-value = 0.04) with TCD measurements.

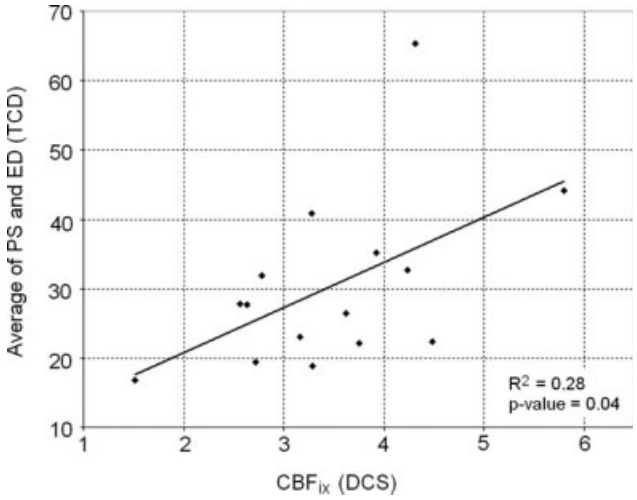

Figure 4.
Scatterplot of the average of PS and ED values (TCD) versus (DCS). The bold line is the linear regression; R^2 and P-value of the regression is in the bottom right corner.

DISCUSSION

This study shows that (1) during the first six weeks of life of premature neonates, HbT and StO_2 decrease while CBV stays stable, and CBF increases, (2) DCS appears a valid technique to measure an index of baseline CBF in neonates, (3) $rCMRO_2$ seems better estimated by combining FD-NIRS and DCS than by assuming a CBV-CBF relationship, questioning the validity of assuming a constant relationship in this population. Because of the reduced variance, only by using the blood flow measure are we able to see increases in $CMRO_2$ during the first six weeks of life.

Our data provide initial quantitative values for the optical hemodynamic assessment of premature neonates during the first six weeks of life, and support the relevance of DCS absolute measures of CBF index along with FD-NIRS for in vivo studies of the neonatal brain.

Interpretation

The stability of CBV and decrease of HbT and StO_2 during the first six weeks of life is consistent with previous results in healthy term and preterm neonates using the same technique during the first six to eight weeks of life [Franceschini et al., 2007]. We believe the decrease in StO_2 (21%) and HbT (31%) are due to the 29% decrease in HGB in our subjects during the same period. This is consistent with the decrease in hematocrit observed during the transition from fetal hemoglobin to adult hemoglobin occurring six to eight weeks after birth [Oski and Naiman, 1982]. The constant CBV suggests that during that period vessels do not dilate to increase volume despite the decrease in red blood cells and oxygen delivery arising from decreased hematocrit.

Additionally, we measured an increase in CBF_{ix} of about 28% during the first six weeks of life, which is consistent with TCD studies of term and premature healthy neonates [Kehrer et al., 2005], basal cerebral artery flow velocity measurements during the first 20 days of life [Bode and Wais, 1988], and SPECT measurements of neonates and infants with transient neurological events [Tokumaru

et al., 1999]. This CBF increase may be an attempt to maintain appropriate brain oxygenation despite the HGB decrease. Indeed, while measured HGB and HbT decrease by 29% and 31%, respectively, during the first six weeks of life, StO_2 decreases only by 21%.

Moreover, the blood flow increase may result from the fact that a decreased HGB and hematocrit reduce blood viscosity and resistance, causing the flow to increase under constant pressure. In microvessels the hematocrit is lower than the measured value in large vessels [Lipowsky et al., 1980]. Assuming an initial hematocrit of 40 in these microvessels and using the values reported in [Pries et al., 1992] for vessel diameters between 50 and 200 μm, a 29% reduction in hematocrit causes a reduction in viscosity of 23–25% and an increase in blood flow of 29–33%. This is close to the 28% increase in CBF_{ix} reported in this article.

The correlation between DCS and TCD measurements shows that DCS is a valid technique to measure an index of baseline CBF in neonates. However the correlation was moderate ($R^2 = 0.28$), even when we tried normalizing CBF_{ix} by the amount of blood cells in tissues for each subject (as blood cells are the main moving scatterer responsible for the DCS signal). This moderate R^2 between TCD and DCS is also reported by [Buckley et al., 2009]. DCS and TCD have different sensitivity mechanisms: TCD is representative of a large artery flow, while DCS is weighted toward smaller vessels because of their higher volume density. Overall, further assessment of DCS is necessary, for example by using absolute Arterial Spin Labeling Magnetic Resonance Imaging (ASL-MRI) measurements.

The interindividual variance of $rCMRO_2$ is far less when combining DCS with NIRS than when using only NIRS and assuming a CBV-CBF relationship with constant β. Considering that our NIRS assessments of HbT and StO_2 evolution during the first six weeks of life are stable across subjects, that these measurements' reproducibility is 11 ± 1% and 4 ± 1%, respectively, and that the same absorption coefficients used to calculate CBV are also used to calculate CBF_{ix}, it is unlikely that this difference comes from an invalid CBV measure. Instead, these results suggest the CBF-CBV relationship may not be valid in premature neonates.

The increase in $rCMRO_2$ resulting from using DCS measures of CBF_{ix} is consistent with electrophysiology showing increasing neuronal activity [Lamblin et al., 1999] and with PET studies showing increasing cortical glucose uptake during the same period [Chugani, 1998; Chugani and Phelps, 1986].

Using Eq. (5) with our values of CBV and CBF_{ix} for all measurements in all subjects, we calculated the average value of β with the assumption of a constant CBV-CBF relationship during this period. This calculation gives $\beta = 0.9 \pm 1.1$, which is not physiologically viable as the minimum value of β is set at 2 by the Poiseuille's Law for laminar flow at fixed pressure (Poiseuille, 1840). This discrepancy in β would be expected if flow changes are arising from reduced vascular resistance due to hematocrit decreases rather than volume increases.

Limitations

Sampled areas

In this study we averaged results from all locations. Because there may be a difference in the pattern of hemodynamic variables among different locations [Chugani and Phelps, 1986; Franceschini et al., 2007], we carried out the same analysis using only frontal, parietal, or temporal recordings. The results did not show any difference between these different locations, justifying averaging them for this study.

Corrected gestational age

We also tested whether averaging data by corrected gestational age (cGA) instead of age would change the patterns of evolution of the variables. Except for a larger interindividual variability for all variables the patterns were similar, suggesting that age is a better predictor of these variables than cGA among our population.

Gestational age

The values of HbT and StO_2 seemed higher in subjects born after 32 wGA, but that difference did not reach significance. Further research involving larger samples is required to investigate this effect.

Treatment

Because premature neonates without any medication or respiratory assistance were few, we had to recruit some patients under treatment. Caffeine is known to increase neural stimulation and decrease CBF, uncoupling CBF and $rCMRO_2$, but its effects on baseline CBV, StO_2 and $rCMRO_2$ remain controversial [Chen and Parrish, 2009; Perthen et al., 2008]. Ventilation modes are also suspected to affect brain hemodynamics, although results are still inconsistent [Milan et al., 2009]. It is unclear how these parameters influenced our data, but as this study is part of a larger prospective study where any neonate in the hospital is eligible for recruitment, we may be able to address these issues in future publications.

CONCLUSION

FD-NIRS combined with DCS offers a safe, highly effective, and quantitative bedside method to track CBV, StO_2, and CBF as well as $rCMRO_2$ in the premature brain. Quantitative values facilitate individual follow-up and comparison among patients. Using DCS measures of CBF instead of CBF estimates based on adult data of the CBV-CBF relationship reduced variation, suggesting that stable

adult values of CBV-CBF relationship may not be accurate in the premature brain.

The ability to safely and routinely monitor premature neonates for regional cerebral development of oxygen utilization, cerebral blood volume (i.e., vascularization) and cerebral blood flow at bedside is of clinical importance as it may allow early detection of abnormal hemodynamics. It is now essential to determine if DCS can also detect brain injuries in infants, as suggested by recent results in the piglet brain [Zhou et al., 2009]. It could then be associated with NIRS detection of brain injury using CBV and $rCMRO_2$ [Grant et al., 2009]. These studies are being planned, as are studies correlating these quantitative NIRS variables with long-term cognitive and behavioral outcomes to determine if they are useful predictors.

ACKNOWLEDGMENTS

The authors thank all the families for their participation in this study and the nurses, physicians, and staff in the Neonatal ICU, the Special Care Nursery, Pediatric Neurology, and the maternity units at Massachusetts General Hospital for helping with recruitment and data collection.

REFERENCES

Altman DI, Powers WJ, Perlman JM, Herscovitch P, Volpe SL, Volpe JJ (1988): Cerebral blood flow requirement for brain viability in newborn infants is lower than in adults. Ann Neurol 24:218–226.

Amiel-Tison C, Grenier A (1986): Neurological Assessment during the First Year of Life. New York: Oxford University Press.

Bayley N (1993): The Bayley Scales of Infant and Toddler Development. New York: Psychological Corporation.

Benaron DA, Benitz WE, Ariagno RA, Stevenson DK (1992): Noninvasive methods for estimating in vivo oxygenation. Clin Pediatrics 31:258–273.

Benaron DA, Ho DC, Spilman S, Van Houten JP, Stevenson DK (1994): Tomographic time-of-flight optical imaging device. Adv Exp Med Biol 361:207–214.

Blankenberg FG, Loh NN, Bracci P, D'Arceuil HE, Rhine WD, Norbash AM, Lane B, Berg A, Person B, Coutant M, Enzmann DR (2000): Sonography, CT, and MR imaging: A prospective comparison of neonates with suspected intracranial ischemia and hemorrhage. Am J Neuroradiol 21:213–218.

Boas DA, Campbell LE, Yodh AG (1995): Scattering and imaging with diffusing temporal field correlations. Phys Rev Lett 75:1855–1859.

Boas DA, Yodh AG (1997): Spatially varying dynamical properties of turbid media probed with diffusing temporal light correlation. J Opt Soc Am 14:192–215.

Bode H, Wais U (1988): Age dependence of flow velocities in basal cerebral arteries. Arch Disease Childhood 63:606–611.

Bozkurt A, Onaral B (2004): Safety assessment of near infrared light emitting diodes for diffuse optical measurements. BioMed Eng OnLine 3:1–10.

Brazy JE, Lewis DV, Mitnick MH (1985): Noninvasive monitoring of cerebral oxygenation in preterm infants: Preliminary observations. Pediatrics 75:217–225.

Brown DW, Hadway J, Lee T-Y (2003): Near-infrared spectroscopy measurement of oxygen extraction fraction and cerebral metabolic rate of oxygen in newborn piglets. Pediatr Res 54:861–867.

Buckley EM, Cook NM, Durduran T, Kim MN, Zhou C, Choe R, Yu G, Schultz S, Sehgal CM, Licht DJ, Arger PH, Putt ME, Hurt HH, Yodh AG (2009): Cerebral monitoring in preterm infants during positional intervention measured with diffuse correlation spectroscopy and transcranial doppler ultrasound. Opt Exp 17:12571–12581.

Carlsson J, Lagercrantz H, Olson L, Printz G, Bartocci M (2008): Activation of the right fronto-temporal cortex during maternal facial recognition in young infants. Acta Paediatr 97:1221–1225.

Chen Y, Parrish TB (2009): Caffeine's effects on cerebrovascular reactivity and coupling between cerebral blood flow and oxygen metabolism. NeuroImage 44:647–652.

Cheung C, Culver JP, Kasushi T, Greenberg JH, Yodh AG (2001): In vivo cerebrovascular measurement combining diffuse near-infrared absorption and correlation spectroscopies. Phys Med Biol 46:2053–2065.

Chugani HT (1998): A critical period of brain development: Studies of cerebral glucose utilization with PET. Prevent Med 27:184–188.

Chugani HT, Phelps ME (1986): Maturational changes in cerebral function in infants determined by 18FDG positron emission tomography. Science 231:840–843.

Culver JP, Durduran T, Cheung C, Furuya D, Greenberg JH, Yodh AG (2003): Diffuse optical measurement of hemoglobin and cerebral blood flow in rat brain during hypercapnia, hypoxia and cardiac arrest. Adv Exp Med Biol 23:293–298.

deAlarcón P, Werner E, editors (2005): Neonatal Hematology. United Kingdom: Cambridge University Press.

Durduran T, Burnett MG, Yu G, Zhou C, Furuya D, Yodh AG, Detre JA, Greenberg JH (2004a): Spatiotemporal quantification of cerebral blood flow during functional activation in rat somatosensory cortex using laser-speckle flowmetry. J Cerebral Blood Flow Metabol 24:518–525.

Durduran T, Choe R, Yu G, Zhou C, Tchou JC, Czerniecki BJ, Yodh AG (2005): Diffuse optical measurements of blood flow in breast tumors. Opt Lett 30:2915–2917.

Durduran T, Yu G, Burnett MG, Detre JA, Greenberg JH, Wang J, Zhou C, Yodh AG (2004b): Diffuse optical measurement of blood flow, blood oxygenation, and metabolism in a human brain during sensorimotor cortex activation. Opt Lett 29:1766–1768.

Edwards AD, Richardson C, Cope M, Wyatt JS, Delpy DT, Reynolds EOR (1988): Cotside measurement of cerebral blood flow in ill infants by near-infrared spectroscopy. The Lancet 332: 770–771.

Elwell CE, Henty JR, Leung TS, Austin T, Meek JH, Delpy DT, Wyatt JS (2005): Measurement of CMRO2 in neonates undergoing intensive care using near infrared spectroscopy. Adv Exp Med Biol 566:263–268.

Fabbri F, Sassaroli A, Henry ME, Fantini S (2004): Optical measurements of absorption changes in two-layered diffusive media. Phys Med Biol 49:1183–1201.

Fantini S, Franceschini M, Maier JS, Walker SA, Barbieri B, Gratton E (1995): Frequency-domain multichannel optical detector for non-invasive tissue spectroscopy and oximetry. Opt Eng 34:34–42.

Franceschini M, Fantini S, Paunescu LA, Maier JS, Gratton E (1998): Influence of a superficial layer in the quantitative spectroscopic study of strongly scattering media. Appl Opt 37: 7447–7458.

Franceschini MA, Thaker S, Themelis G, Krishnamoorthy KK, Bortfeld H, Diamond SG, Boas DA, Arvin K, Grant PE (2007): Assessment of infant brain development with frequency-domain near-infrared spectroscopy. Pediatr Res 61:546–551.

Grant PE, Roche-Labarbe N, Surova A, Themelis G, Selb J, Warren EK, Krishnamoorthy KK, Boas DA, Franceschini M (2009): Increased cerebral blood volume and oxygen consumption in neonatal brain injury. J Cerebral Blood Flow Metabolism (in press).

Grubb RLJ, Raichle ME, Eichling JO, Ter-Pogossian MM (1974): The effects of changes in PaCO2 on cerebral blood volume, blood flow, and vascular mean transit time. Stroke 5:630–639.

Hamaoka T, Katsumura T, Murase N, Nishio S, Osada T, Sako T, Higuchi H, Kurosawa Y, Shimomitsu T, Miwa M, Chance B (2000): Quantification of ischemic muscle deoxygenation by near infrared time-resolved spectroscopy. J Biomed Opt 5:102–105.

Hebden JC, Gibson AP, Yusof RM, Everdell N, Hillman EMC, Delpy DT, Arridge SR, Austin T, Meek JH, Wyatt JS (2002): Three-dimensional optical tomography of the premature infant brain. Phys Med Biol 47:4155–4166.

Ijichi S, Kusaka T, Isobe K, Okubo K, Kawada K, Namba M, Okada H, Nishida T, Imai T, Itoh S (2005): Developmental changes of optical properties in neonates determined by near-infrared time-resolved spectroscopy. Pediatr Res 58:568–573.

Ito Y, Kennan RP, Watanabe E, Koizumi H (2000): Assessment of heating effects in skin during continuous wave near infrared spectroscopy. J Biomed Opt 5:383–391.

Kehrer M, Blumenstock G, Ehehalt S, Goelz R, Poets C, Schöning M (2005): Development of cerebral blood flow volume in preterm neonates during the first two weeks of life. Pediatr Res 58:927–930.

Kellaway P (2003): Orderly approach to visual analysis: Elements of the normal eeg, and their characteristics in children and adults. In: Ebersole JS, Pedley TA, editors. Current Practice of Clinical Electroencephalography. Philadelphia: Lippincott Williams & Wilkins. pp 100–159.

Kiechl-Kohlendorfer U, Ralser E, Peglow UP, Reiter G, Trawöger R (2009): Adverse neurodevelopmental outcome in preterm infants: Risk factor profiles for different gestational ages. Acta Paediatr 98:792–796.

Kirkpatrick SJ, Duncan DD, Wells-Gray EM (2008): Detrimental effects of speckle-pixel size matching in laser speckle contrast imaging. Opt Lett 33:2886–2888.

Kretschmann HJ, Kammradt G, Krauthausen I, Sauer B, Wingert F (1986): Brain growth in man. Bibliotheca Anatomica 28:1–26.

Lamblin MD, André M, Challamel MJ, Curzi-Dascalova L, d'Allest AM, De Giovanni E, Moussalli-Salefranque F, Navelet Y, Plouin P, Radvanyi-Bouvet MF, Samson-Dollfus D, Vecchierini-Blineau MF (1999): Electroencephalography of the premature and term newborn. Maturational aspects and glossary. Neurophysiol Clin 29:123–219.

Leung TS, Aladangady N, Elwell CE, Delpy DT, Costeloe K (2004): A new method for the measurement of cerebral blood volume and total circulating blood volume using near infrared spatially resolved spectroscopy and indocyanine green: Application and validation in neonates. Pediatr Res 55:134–141.

Li J, Dietsche G, Iftime D, Skipetrov SE, Maret G, Elbert T, Rockstroh B, Gisler T (2005): Noninvasive detection of functional brain activity with near-infrared diffusing-wave spectroscopy. J Biomed Opt 10:044002.

Lipowsky HH, Usami S, Chien S (1980): In vivo measurements of "apparent viscosity" and microvessel hematocrit in the mesentery of the cat. Microvasc Res 19:297–319.

Marret S, Foix-L'hélias L, Ancel PY, Kaminski M, Larroque B, Marcou-Labarre A, Laudenbach V (2008): Is it possible to protect the preterm infant brain and to decrease later neurodevelopmental disabilities? Archives de Pédiatrie 15(Suppl 1):S31–S41.

Martin JA, Hamilton BE, Sutton PD, Ventura SJ, Menacker F, Kirmeyer S, Mathews TJ (2009): Births: Final Data for 2006. National Center for Health Statistics.

Meek JH, Tyszczuk L, Elwell CE, Wyatt JS (1998): Cerebral blood flow increases over the first three days of life in extremely preterm neonates. Archives of Disease in Childhood. Fetal and Neonatal Edition 78, F33-F37.

Milan A, Freato F, Vanzo V, Chiandetti L, Zaramella P (2009): Influence of ventilation mode on neonatal cerebral blood flow and volume. Early Hum Dev 85:415–419.

Nicklin SE, Hassan IA-A, Wickramasinghe YA, Spencer SA (2003): The light still shines, but not that brightly? The current status of perinatal near infrared spectroscopy. Arch Disease Childhood Fetal Neonatal Ed 88:263–268.

Noone MA, Sellwood M, Meek JH, Wyatt JS (2003): Postnatal adaptation of cerebral blood flow using near infrared spectroscopy in extremely preterm infants undergoing high-frequency oscillatory ventilation. Acta Paediatrica 92:1079–1084.

Oski FA, Naiman JL (1982): Hematologic problems in the newborn. Third edition. Major Problems Clin Pediatr 4:1–360.

Patel J, Marks K, Roberts I, Azzopardi D, David EA (1998): Measurement of cerebral blood flow in newborn infants using near infrared spectroscopy with indocyanine green. Pediatr Res 43:34–39.

Perlman JM (2006): Summary proceedings from the neurology group on hypoxic-ischemic encephalopathy. Pediatrics 117 (Part 2): S28–S33.

Perthen JE, Lansing AE, Liau J, Liu TT, Buxton RB (2008): Caffeine-induced uncoupling of cerebral blood flow and oxygen metabolism: A calibrated BOLD fMRI study. NeuroImage 40:237–247.

Peterson BS, Anderson AW, Ehrenkranz R, Staib LH, Tageldin M, Colson E, Gore JC, Duncan CC, Makuch R, Ment LR (2003): Regional brain volumes and their later neurodevelopmental correlates in term and preterm infants. Pediatrics 111:939–948.

Pries AR, Neuhaus D, Gaehtgens P (1992): Blood viscosity in tube flow: Dependence on diameter and hematocrit. Am J Physiol 263(Part 2):H1770–H1778.

Shellhaas RA, Soaita AI, Clancy R (2007): Sensitivity of amplitude-integrated electroencephalography for neonatal seizure detection. Pediatrics 120:770–777.

Skov L, Pryds O, Greisen G, Lou H (1993): Estimation of cerebral venous saturation in newborn infants by near infrared spectroscopy. Pediatr Res 33:52–55.

Takahashi T, Shirane R, Sato S, Yoshioto T (1999): Developmental changes of cerebral blood flow and oxygen metabolism in children. Am J Neuroradiol 20:917–922.

Tokumaru AM, Barkovich AJ, O'Uchi T, Matsuo T, Kusano S (1999): The evolution of cerebral blood flow in the developing brain: Evaluation with iodine-123 iodoamphetamine SPECT and correlation with MR imaging. AJNR. Am J Neuroradiol 20:845–852.

Watanabe H, Homae F, Nakano T, Taga G (2008): Functional activation in diverse regions of the developing brain of human infants. Neuroimage 43:346–357.

Watzman HM, Kurth CD, Montenegro LM, Rome J, Steven JM, Nicolson SC (2000): Arterial and venous contributions to near-infrared cerebral oximetry. Anesthesiology 93:947–953.

Wolff JA, Goodfellow AM (1955): Hematopoiesis in premature infants with special consideration of the effect of iron and of animal-protein factor. Pediatrics 16:753–762.

Wolthuis R, van Aken M, Fountas K, Robinson JSJ, Bruining HA, Puppels GJ (2001): Determination of water concentration in brain tissue by Raman spectroscopy. Anal Chem 73:3915–3920.

Wray S, Cope M, Delpy DT, Wyatt JS, Reynolds EO (1988): Characterization of the near infrared absorption spectra of cytochrome aa3 and haemoglobin for the non-invasive monitoring of cerebral oxygenation. Biochimica et biophysica acta 933:184–192.

Wyatt JS, Cope M, Delpy DT, Wray S, Reynolds EO (1986): Quantification of cerebral oxygenation and haemodynamics in sick newborn infants by near infrared spectrophotometry. Lancet 2:1063–1066.

Yoxall CW, Weindling AM (1998): Measurement of cerebral oxygen consumption in the human neonate using near infrared spectroscopy: Cerebral oxygen consumption increases with advancing gestational age. Pediatr Res 44:283–290.

Yu G, Durduran T, Lech G, Zhou C, Chance B, Mohler ER III, Yodh AG (2005): Time-dependent blood flow and oxygenation in human skeletal muscles measured with noninvasive near-infrared diffuse optical spectroscopies. J Biomed Opt 10:024027-1–12.

Zaramella P, Saraceni E, Freato F, Falcon E, Suppiej A, Milan A, Laverda AM, Chiandetti L (2007): Can tissue oxygenation index (TOI) and cotside neurophysiological variables predict outcome in depressed/asphyxiated newborn infants?Early Hum Dev 83:483–489.

Zhao J, Ding HS, Hou XL, Zhou CL, Chance B (2005): In vivo determination of the optical properties of infant brain using frequency-domain near-infrared spectroscopy. J Biomed Opt 10:024028.

Zhou C, Choe R, Shah N, Durduran T, Yu G, Durkin A, Hsiang D, Mehta R, Butler J, Cerussi A, Tromberg BJ, Yodh AG (2007): Diffuse optical monitoring of blood flow and oxygenation in human breast cancer during early stages of neoadjuvant chemotherapy. J Biomed Opt 12:051903–051903.

Zhou C, Eucker SA, Durduran T, Yu G, Ralston J, Friess SH, Ichord RN, Margulies SS, Yodh AG (2009): Diffuse optical monitoring of hemodynamic changes in piglet brain with closed head injury. J Biomed Opt 14:034015.